

Dynamical Structure Factor in Warm Dense Matter and Applications to X-Ray Thomson Scattering

Carsten Fortmann

Lawrence Livermore National Laboratory
University of California Los Angeles

IPAM, May 24, 2012



This work performed under the auspices of the U.S. Department of Energy

by Lawrence Livermore National Laboratory under Contract DE-AC52-07NA27344.

Contributors



S. H. Glenzer, T. Döppner, A. L. Kritcher, O. N. Landen, T. Ma, A. Pak



R. Redmer, K.-U. Plagemann, P. Sperling, G. Röpke A. Wierling

UCLA Ch. Niemann



P. Davis, L. Fletcher, R. Falcone

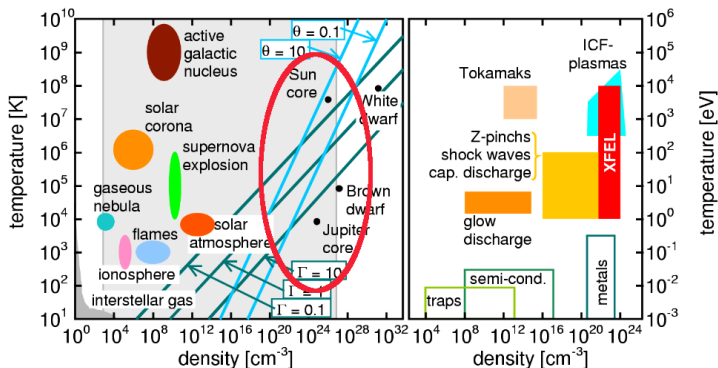


H. J. Lee

SNL M. Desjarlais

- Introduction: X-Ray diagnostics of WDM
- Many-body theory of light-matter interaction
- The Dynamical Structure Factor
- Semi-analytic calculations of structure factors in WDM
- Applications: X-ray scattering from warm dense plasmas
- Ab-initio calculations for the dynamical structure factor
- Summary and Conclusions

Studying matter under extreme conditions is relevant to understand astrophysical and laboratory plasmas

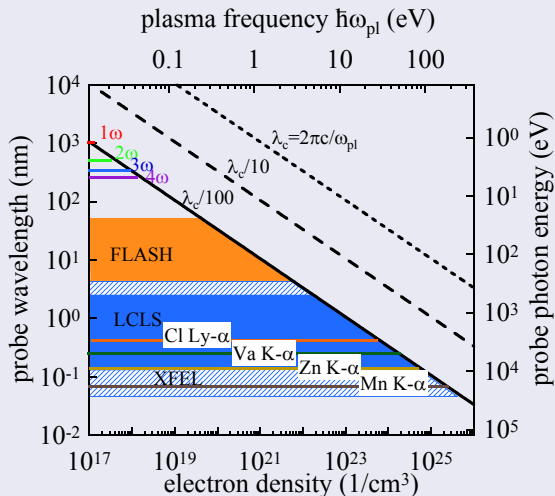


- Plasma parameters:

- Coupling parameter $\Gamma = \frac{Ze^2}{4\pi\epsilon_0 k_B T} \left(\frac{4\pi n}{3} \right)^{1/3}$
- Degeneracy parameter $\theta = \frac{k_B T}{E_F}$, $E_F = \frac{\hbar^2}{2m} (3\pi n)^{2/3}$

Probing the bulk properties of solid density plasmas requires intense x-ray sources

Critical wavelength vs. electron density



- X-rays penetrate deep into solid matter
- volumetric heating possible, mitigate n_e/T gradients
- probe bulk properties of dense matter, discard surface effects
- **Need accurate theory for the interaction of correlated matter with x-rays**

The QED Lagrangian governs the particle and field dynamics

$$\mathcal{L}(x) = \sum_c \bar{\psi}_c(x) (i\hbar c \gamma^\mu \partial_\mu - m_c c^2) \psi_c(x) - \frac{\epsilon_0 c^2}{4} F_{\mu\nu}(x) F^{\mu\nu}(x) + \sum_c Z_c e j_{\mu c}(x) A^\mu(x)$$

- Free fermions, Dirac equation, particle current $j_{\mu c} = \bar{\psi}_c(x) \gamma_\mu \psi_c(x)$
- Free gauge fields, Maxwell equations, fields $F_{\mu\nu} = \partial^\mu A^\nu(x) - \partial^\nu A^\mu(x)$
- minimal particle-field coupling
⇒ emission/absorption, collisions, radiative damping

The current-current correlation gives the linear response to external fields (EM, pressure, particles)

4-current dynamical structure factor $S_{\mu\nu}(k)$

$$S_{\mu\nu}(k) = \int d^4x' \exp(ik_\lambda x'^\lambda) \langle j_\mu^\dagger(x+x') j_\nu(x) \rangle_x \quad k = (\omega/c, \vec{k}), \quad x = (ct, \vec{x})$$

Correlation functions are expressed via Green functions

$$\langle j_\mu^\dagger j_\nu \rangle_k = \frac{1}{\pi} \text{Im} G_{jj}(k)$$

Green functions are systematically evaluated using MB Feynman diagrams

$$G_{jj}(k) = \text{Diagram}$$

Dyson-Schwinger Equations

Fermion propagator $G = G^{(0)} + G^{(0)} \Sigma G$

Self-energy: $\Sigma = \text{wavy loop}$ QP shift+damping (lifetime)

Field propagator: $W = V + V \Pi W$

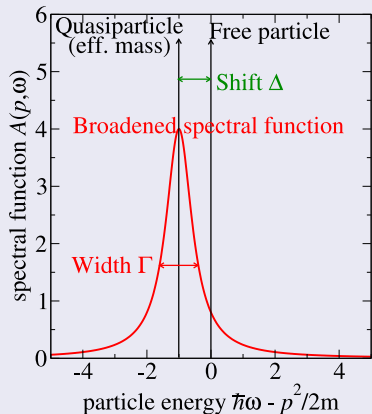
Polarization: $\Pi = \text{fermion loop}$ Dynamical screening

Vertex: $\text{fermion-fermion-wavy vertex} = \text{fermion-fermion-wavy vertex} + \text{fermion-fermion-wavy vertex} \text{ with } K \text{ box}$ eff. coupling

Dyson, *Phys. Rev.* **75** (1949), Schwinger, *PNAS* **37** (1951)

Hedin, *Phys. Rev.* **139** (1965)

The spectral function describes damped quasiparticles in a dense medium



$$A(\vec{p}, \omega) = -2\text{Im} G(\vec{p}, \omega + i0^+)$$

- $A(\vec{p}, \omega)$: probability for particle with momentum \vec{p} at energy $\hbar\omega$.

- Free particle:

$$A^{\text{FP}}(\vec{p}, \omega) = 2\pi \delta(\hbar\omega - p^2/2m)$$

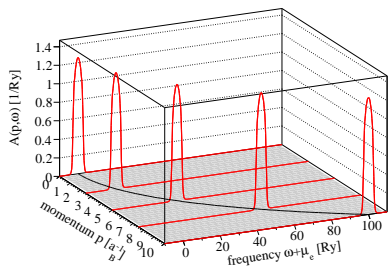
- Dense medium:

$$A(\vec{p}, \omega) = \frac{-2\Gamma(\vec{p}, \omega)}{[\hbar\omega - E_p - \Delta(\vec{p}, \omega)]^2 + [\Gamma(\vec{p}, \omega)]^2}$$

$$\Sigma(\vec{p}, \omega) = \Delta(\vec{p}, \omega) + i\Gamma(\vec{p}, \omega)$$

Example: GW_0 spectral function

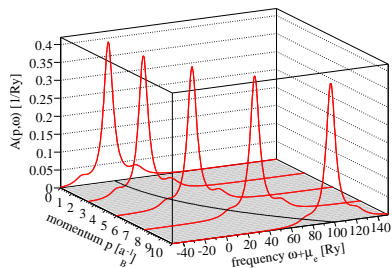
Spectral function for dilute plasma ($n_e = 10^{22}/cc$, $T = 1$ keV)



- Narrow width, ideal dispersion
- No quasiparticle satellites

Fortmann, J.Phys.A (2008) & PRE (2009)

Spectral function for dense plasma ($n_e = 10^{26}/cc$, $T = 1$ keV)



- Strongly damped & shifted
- Plasmaron satellites

The spectral function yields important observables

Equation of state

$$n_a(\mu_a, T) = \int_{-\infty}^{\infty} \frac{d\omega}{2\pi} \int \frac{d^3p}{(2\pi)^3} f_a(\omega) A_a(\vec{p}, \omega)$$

Vorberger et al. PRE 69, 046407 (2004)

Band structure

$$E_p = \hbar^2 p^2 / 2m + \text{Re} \Sigma(\vec{p}, E_p)$$

Optical properties

$$\Pi_e(\vec{k}, \omega_\mu) = \sum_{z_\nu, \vec{p}} \int_{-\infty}^{\infty} \frac{d\omega}{2\pi} \frac{d\omega'}{2\pi} \Gamma_0 \frac{A_e(\vec{p} + \vec{k})}{\omega - z_\nu - \omega_\mu} \frac{A_e(\vec{p}, \omega')}{\omega' - z_\nu} \Gamma(\omega_\mu + z_\nu, z_\nu; \vec{p} + \vec{k}, \vec{p})$$

Fortmann et al., Contrib. Plasma Phys. 94 (2007)

Bremsstrahlung

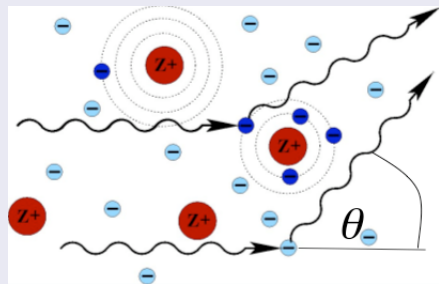
- $\sigma_{\text{brems}}(\vec{k}, \omega) \propto \text{Im} \Pi_{ee}(\vec{k}, \omega)$
- Important energy loss/heating process in dense plasmas
- Spectrum typically $\propto e^{-\hbar\omega/k_B T}$
 \Rightarrow Temperature diagnostic for hot electrons
- Direct measure of collisionality in the plasma
- Electron distribution function can be calculated by deconvolution of spectrum from elementary cross-section

Inelastic x-ray scattering

- $\sigma_{IXS}(\vec{k}, \omega) \propto S_{00}^{ee}(\vec{k}, \omega)$
- Important $n_e, T, Z_f, \rho/\rho_0$ diagnostic
- Sensitive to many-body correlations (collisions, local field effects)
- Spectrum gives information about free-free, bound-free, and bound-bound correlations

X-ray scattering is a versatile dense matter diagnostic tool

A diagnostic for complex systems

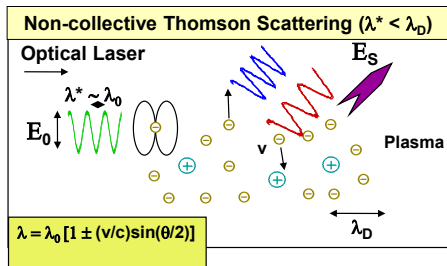


- scattering from free and bound electrons
- sensitive to static and dynamic correlations
- e-e and e-i interaction
- strongly non-ideal system

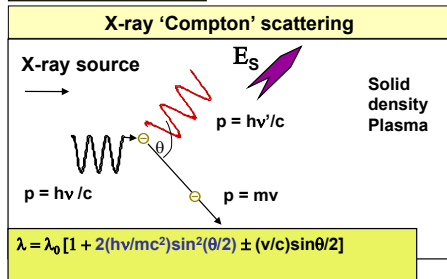
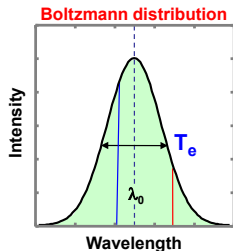
Key advantages of x-ray scattering

- undercritical for solids and compressed matter
- deep penetration
- probe bulk properties
- measures both dynamic and static plasma properties
- direct n_e , T_e measurement via first principle relations (plasma frequency, detailed balance)
- high spatial and temporal resolution thanks to modern x-ray sources (backlighters, fel's)

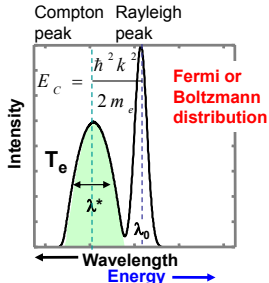
Scattering spectrum reflects the correlation of density fluctuations



Scattering on free electrons



Scattering on free and weakly bound electrons



XRTS resolves collective and single particle dynamics

Scattering Parameter: α

$$\alpha = \frac{1}{k\lambda_s} \propto \frac{\lambda}{\lambda_s}$$

$$k = \frac{4\pi}{\lambda_o} \sin(\theta/2)$$

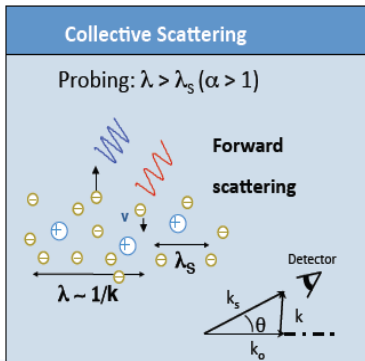
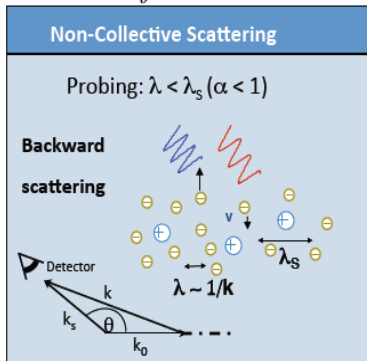
Plasma Screening Length: λ_s

Fermi-degenerate Plasma:

$$\lambda_{TF} = \left(\frac{\hbar^2}{4m_e e^2} \left(\frac{\pi}{3n_e} \right)^{1/3} \right)^{1/2}$$

Classical Plasma:

$$\lambda_D = \left(\frac{\epsilon_0 k T_e}{n_e e^2} \right)^{1/2}$$



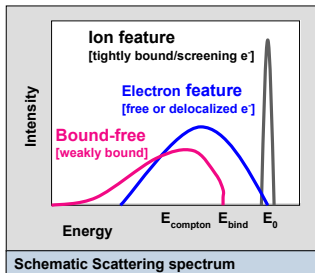
Dynamical Structure Factor $S(\vec{k}, \omega)$

Scattered power P_s per frequency interval $d\omega$ per solid angle $d\Omega$

$$P_s(\vec{R}, \omega) d\Omega d\omega = \frac{P_i r_0^2 d\Omega}{2\pi A} \left| \hat{\vec{k}}_f \times (\hat{\vec{k}}_f \times \hat{\vec{E}}_{0i}) \right|^2 N S(\vec{k}, \omega) d\omega$$
$$S(\vec{k}, \omega) = \frac{1}{2\pi N} \int dt e^{i\omega t} \langle \rho_e(\vec{k}, t) \rho_e(-\vec{k}, 0) \rangle$$

- S : density-density correlation function \Leftrightarrow coherent superposition of density fluctuations
- S determined via
 - scattering experiments
 - theoretical calculations
 - computer simulations (MD, QMD, WPMD, ...)
- $r_0 = e^2/4\pi\epsilon_0 m_e c^2$: classical electron radius
- N : number of scattering centers; A : area of illuminated plasma
- $\left| \hat{\vec{k}}_f \times (\hat{\vec{k}}_f \times \hat{\vec{E}}_{0i}) \right|^2$: laser polarization

$$S(\mathbf{k}, \omega) = |f_l(k) + q(k)|^2 S_{ii}(\mathbf{k}, \omega) + Z_f S_{ee}^0(\mathbf{k}, \omega) + Z_c S_{core}(\mathbf{k}, \omega)$$



- $f(k)$: ionic form factor, elastic scattering from bound states
- $q(k)$: “screening cloud”: free electrons following ions adiabatically
- $S_{ii}(k, \omega)$: ion-ion structure factor
- $S_{ee}^0(k, \omega)$: Electron OCP structure factor (e.g. plasmons)
- $S_{core}(k, \omega) \propto \langle \vec{p} | e^{i\vec{k}\cdot\vec{r}} | nlm \rangle$: bound-free scattering

Electronic subsystem

- $e - e$ correlations important at finite k
- treat e correlations via LFC

$$\rightarrow \chi_{ee}^{\text{OCP}} = \frac{\chi_e^{(0)}}{1 - V(1 - G_{ee})\chi_e^{(0)}}$$

Ionic subsystem

- static structure factor $S_{ii}(k)$
- e.g. HNC, DFT-MD

Wünsch et al. PRE (2009)

Schwarz et al., HEDP (2010)

Coupling of e and i subsystems

- $e - i$ collision frequency

$$\nu^{\text{Born}}(\omega) \propto \frac{Z_f}{\omega} \int_0^\infty dq q^6 V_S^2(q) S_{ii}(q) \left[\chi^{(0)}(q, \omega) - \chi^{(0)}(q, 0) \right]$$

- Mermin ansatz with correlated electrons and $e - i$ collision frequency

$$\chi^{\text{xM}}(k, \omega) = \frac{-iz}{\nu(\omega)} \frac{\chi^{\text{OCP}}(k, z) \chi^{\text{OCP}}(k, 0)}{\chi^{\text{OCP}}(k, z) - \frac{i\omega}{\nu(\omega)} \chi^{\text{OCP}}(k, 0)}, z = \omega + i\nu(\omega)$$

Fortmann et al, PRE 81 (2010)

relevant statistical operator for multi-component plasma

Zubarev et al. *Statistical Mechanics of Nonequilibrium Processes* (1996)

$$\rho_{\text{rel}} = \exp \left\{ -\Phi(t) - \beta H + \beta \sum_c \mu_c N_c + \beta \sum_c \delta \mu_c(k, \omega) n_k^c e^{i\omega t} + \text{c.c.} \right\}$$

Lagrange multipliers $\beta, \mu, \delta \mu_c(k, \omega)$ from self-consistency relations

Mermin response function

Mermin, PRB (1970)

Röpke et al., Phys. Lett. A (1999)

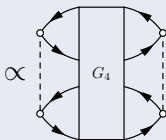
$$\chi_c^{\text{M}}(k, \omega) = \frac{iz}{\nu} \frac{\chi_c^{(0)}(k, z) \chi_c^{(0)}(k, 0)}{\chi_c^{(0)}(k, z) - \frac{i\omega}{\nu} \chi_c^{(0)}(k, 0)}, \quad z = \omega + i\nu(\omega).$$

- χ^{M} conserves local density
- $\nu(\omega)$: dynamical collision frequency, describes e-i collisions

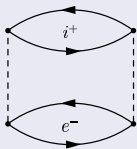
Calculation of the collision frequency

Force-force correlation function

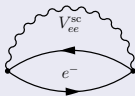
$$\nu(\omega) = \frac{\beta\Omega_0}{\epsilon_0\omega_{pl}^2} \langle j_0^z, j_0^z \rangle_{\omega+i\eta} \propto$$



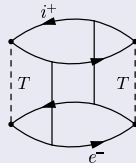
Approximations



Born approximation



Dynamical screening



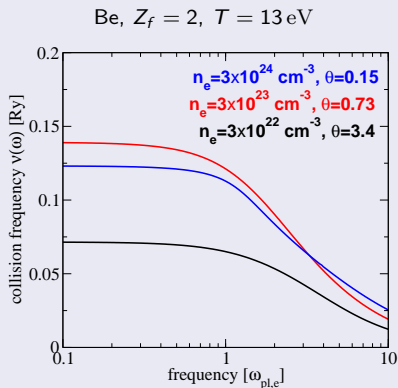
T-matrix

Collision frequency in Born approximation

Redmer et al., IEEE Trans. Plasma Sci (2005)

Fortmann et al., Laser Particle Beams (2009)

$$\nu^{\text{Born}}(\omega) \propto \frac{Z_f}{\omega} \int_0^\infty dq q^6 V_S^2(q) S_{ii}(q) [\epsilon_e^{\text{RPA}}(q, \omega) - \epsilon_e^{\text{RPA}}(q, 0)]$$



- Collisions most important near $\theta = \frac{k_B T}{E_F} \simeq 1$
- At high & low degeneracy Landau damping dominates.
- Inclusion of dynamical screening and strong collisions is straightforward.

Thiele et al., J. Phys. A (2006)

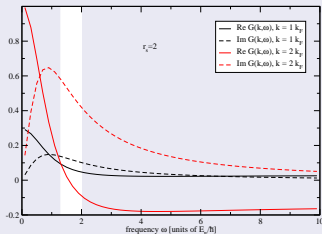
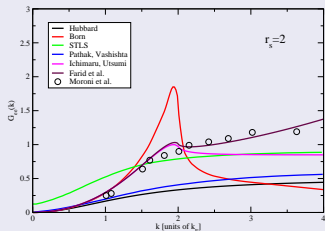
Treatment of e-e correlations via local field corrections (LFC)

$$\chi^{\text{XM}}(\vec{k}, \omega) = \frac{-iz}{\nu(\omega)} \frac{\chi^{\text{OCP}}(\vec{k}, z) \chi^{\text{OCP}}(k, 0)}{\chi^{\text{OCP}}(\vec{k}, z) - \left(\frac{i\omega}{\nu(\omega)}\right) \chi^{\text{OCP}}(\vec{k}, 0)}, \quad z = \omega + i\nu(\omega)$$

$$\chi^{\text{OCP}}(\vec{k}, \omega) = \frac{\chi_e^0(\vec{k}, \omega)}{1 - V_{ee}(k)(1 - G_{ee}(\vec{k}, \omega))\chi_e^0(\vec{k}, \omega)}$$

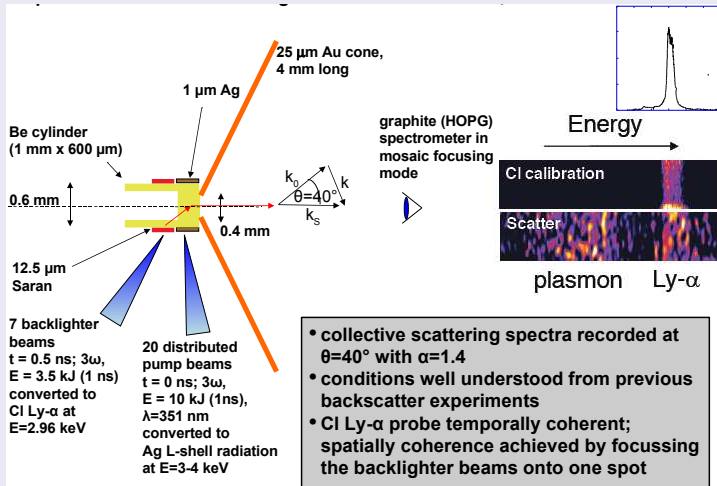
The LFC is calculated using Padé interpolation between low and high ω limits

Wierling et al. *OPF* 2011

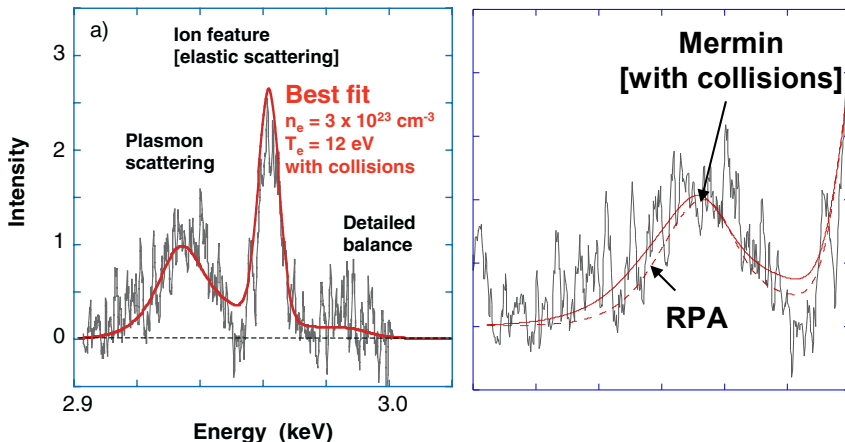


1) XRTS in isochorically heated Be

Glenzer et al., PRL 98, 065002 (2007)



Collisions are crucial to fit the scattering spectrum



Glenzer et al., PRL 98 (2007)

- BMA: $T_e = 12 \text{ eV}$ (consistent w/ independent measurement)
- RPA-fit: $T_e \simeq 30 \text{ eV}$.
- First experimental evidence for the importance of collisions in X-ray plasma scattering.

Fluctuation-dissipation theorem

$$S_{ee}(\vec{k}, \omega) = -\frac{\hbar}{\pi n_e} \text{Im} \chi_{ee}(\vec{k}, \omega)$$

Dyson equations for pair correlation function and screened potential

$$\chi_{cc'}(\vec{k}, \omega) = \chi_c^0(\vec{k}, \omega) \delta_{cc'} + \sum_{d=e,i} \chi_c^0(\vec{k}, \omega) V_{cd}^{sc}(\vec{k}, \omega) \chi_{dc'}(\vec{k}, \omega)$$

$$V_{cc'}^{sc}(\vec{k}, \omega) = V_{cc'}(\vec{k}) + \sum_{d=e,i} V_{cd}(\vec{k}) \chi_d^0(\vec{k}, \omega) V_{dc'}^{sc}(\vec{k}, \omega)$$

$$V_{cc'}(\vec{k}) = \frac{q_c q_{c'}}{\epsilon_0 k^2} \quad (\text{fully ionized, replace by eff. potential in partially ionized plasma})$$

$$\chi_c^0(\vec{k}, \omega) = \text{Diagram} = \frac{1}{\Omega_0} \sum_{\vec{p}} \frac{f_{\vec{p}+\vec{k}/2}^c - f_{\vec{p}-\vec{k}/2}^c}{E_{\vec{p}+\vec{k}/2}^c - E_{\vec{p}-\vec{k}/2}^c - \hbar\omega}$$

Terminate Dyson series after 1st iteration

$$\chi_{cc'}^{RPA}(\vec{k}, \omega) = \chi_c^0(\vec{k}, \omega) \delta_{cc'} + \chi_c^0(\vec{k}, \omega) V_{cc'}^{sc}(\vec{k}, \omega) \chi_{c'}^0(\vec{k}, \omega)$$

Solution to linearized Dyson equations

$$\chi_{ee}^{RPA}(\vec{k}, \omega) = \frac{\chi_e^0 - \chi_e^0 V_{ii} \chi_i^0}{1 - V_{ee} \chi_e^0 - V_{ii} \chi_i^0} \quad \chi_{ei}^{RPA}(\vec{k}, \omega) = \frac{2\chi_e^0 V_{ei} \chi_i^0}{1 - V_{ee} \chi_e^0 - V_{ii} \chi_i^0}$$
$$\chi_{ie}^{RPA}(\vec{k}, \omega) = \chi_{ei}^{RPA}(\vec{k}, \omega) \quad \chi_{ii}^{RPA}(\vec{k}, \omega) = \frac{\chi_i^0 - \chi_i^0 V_{ee} \chi_e^0}{1 - V_{ee} \chi_e^0 - V_{ii} \chi_i^0}$$

Calculation of the DSF

Apply fluctuation dissipation theorem

$$\text{Im } \chi_{ee} = \text{Im } \chi_{ee}^0 + V_{ei}^2 \left\{ \left[(\text{Re } \chi_{ee}^0)^2 - (\text{Im } \chi_{ee}^0)^2 \right] \text{Im } \chi_{ii} + \right. \\ \left. + 2 \text{Re } \chi_{ee}^0 \text{Im } \chi_{ee}^0 \text{Re } \chi_{ii} \right\} \quad \chi_{ee}^0 = \frac{\chi_e^0}{1 - V_{ee} \chi_e^0}$$

Compare to “Chihara formula” (fully ionized case)

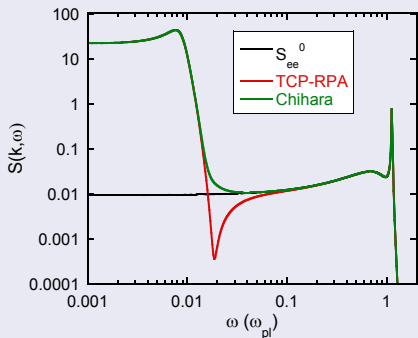
J. Chihara, *J. Phys. Cond. Mat.* (2000)

$$S_{ee}(\mathbf{k}, \omega) = Z_f S_{ee}^0(\mathbf{k}, \omega) + |q(k)|^2 S_{ii}(\mathbf{k}, \omega)$$

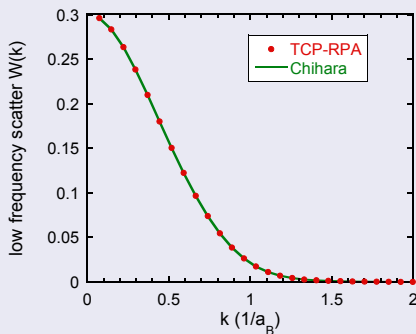
- Identified high frequency component $Z_f S_{ee}^0$ and screening cloud $q(k)$ in TCP-RPA model
- TCP-RPA contains additional dynamic terms

TCP-RPA model largely agrees with Chihara formula

DSF calculations for fully ionized H, $n_e = 10^{22} \text{ cm}^{-3}$, $T = 1 \text{ eV}$



Dynamical structure factor for H,
 $Z_f = 1$, $\alpha = 3$

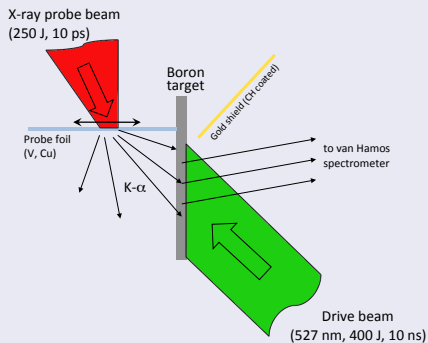


Integrated low frequency signal

- Chihara DSF evaluated in RPA, $q(k) = \sqrt{Z_f} S_{ei}(k) / S_{ii}(k)$
- Additional dynamical features not important for integrated signal

Application 2: Angle and energy resolved XRTS on shock compressed boron

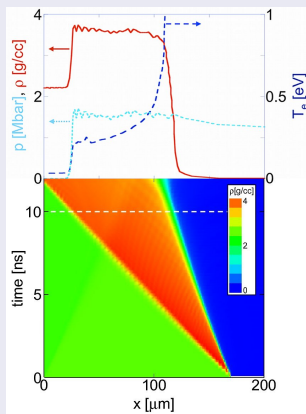
5 and 8 keV photons are used to probe shock-compressed B at various k



Experiments performed at the Titan Laser, LLNL

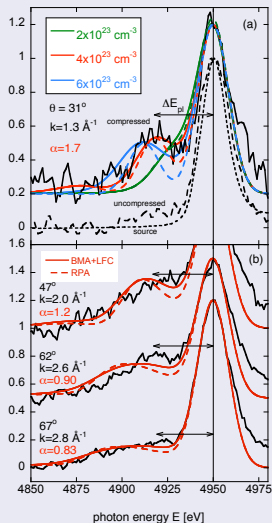
Neumayer, Fortmann et al., PRL (2010)

HELIOS simulations of the drive-beam target interaction

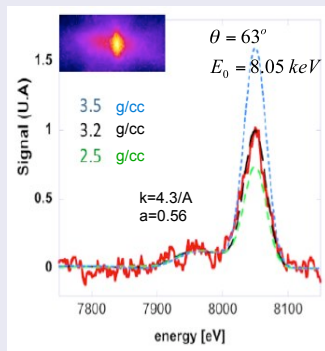


We completely characterize the plasma via XRTS

Plasmon position gives electron density
solid: w/ collisions, dashed: w/o coll.



Non-collective spectrum sensitive to ionization

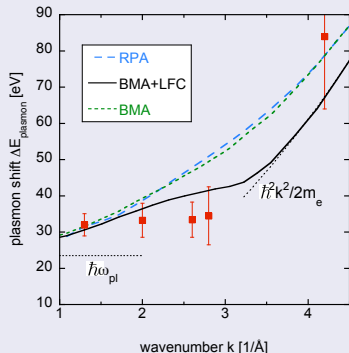


Best fit parameters:

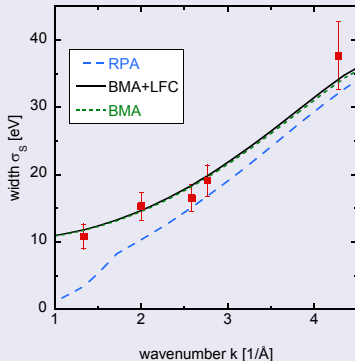
$$n_e = 4 \times 10^{23} \text{ cm}^{-3}, Z_{\text{free}} = 2.3, \Rightarrow \rho/\rho_0 = 1.3. .$$

Plasmon dispersion and width reveal influence of many-particle correlations

Plasmon dispersion data support static LFC model



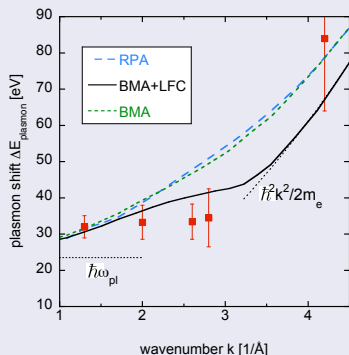
Collisional plasmon width mainly due to e-i collisions



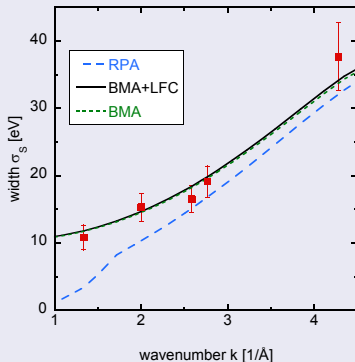
- Still unresolved discrepancies between experiment and theory.

Plasmon dispersion and width reveal influence of many-particle correlations

Plasmon dispersion data support static LFC model



Collisional plasmon width mainly due to e-i collisions



- Still unresolved discrepancies between experiment and theory.

Summary

- Many-body field theory is applied to calculate radiation effects in strongly coupled, non-ideal plasmas.
- Dyson-Schwinger Equations are solved self-consistently yielding the quasi-particle shift and damping
- We developed a reliable Thomson scattering code as a basis for XRTS plasma diagnostics
- Collisional plasmon width and dispersion are successfully described via the extended Born-Mermin approximation.
- First attempts to apply ab-initio methods for DSF calculations are promising